JOURNAL OF MATERIALS SCIENCE 22 (1987) 149–154

Numerical solutions for diffusion-controlled growth of spheres from finite initial size

M. CABLE, J. R. FRADE
Department of Ceramics Glasses and Polymers, University of Sheffield, Northumberland Road, Sheffield S10 2TZ, UK

Efficient numerical methods have been developed to predict the diffusion-controlled growth of an isolated sphere of finite initial size in conditions of spherical symmetry. Analytical solutions for growth from zero size have also been re-examined and it is shown that Scriven's assumption of constant density is unnecessary; it is only required that the partial molar volumes of solute and solvent be independent of concentration. Detailed comparisons of analytical predictions and numerical results for both size and concentration profile confirm the accuracy of the numerical techniques for wide ranges of the parameters concerned.

1. Introduction

Growth or dissolution of particles, drops or bubbles is important in many chemical and physical processes. Particular cases may be influenced by many factors but solution of even the simplest case, diffusion-controlled growth or dissolution of an isolated sphere with spherical symmetry, constant diffusivity and constant conditions at the interface, offers sufficient challenge to deserve thorough study.

An analytical solution for heat conduction in a region bounded internally by a sphere has long been available (Carslaw and Jaeger [1]) but cannot properly allow for either change in the size of the sphere or radial convection in the surrounding medium that may accompany change in size of the sphere. Frank [2] showed that analytical solutions for growth from zero size can be obtained when the volume of the system is constant and there is no convective flow in the liquid outside the sphere, if transient effects are neglected. Frank's solution is a reasonable approximation for many examples involving solids but not for other cases such as gas bubbles. Scriven [3] considerably extended the model for growth from zero size by again assuming the existence of a self-similar concentration profile but allowing for a change in volume as solute was transferred across the interface, although still assuming constant density for the liquid outside the sphere.

Dealing with the growth or dissolution of a sphere of finite initial size increases the difficulty of finding solutions. Several authors have used approximate solutions, for example Epstein and Plesset [4], Cable [5] and Doremus [6], whilst others, such as Readey and Cooper [7], Cable and Evans [8] and Duda and Vrentas [9], have solved the differential equations numerically, but their methods were not properly tested against exact solutions where such tests were possible. The present authors are especially interested in predicting the behaviour of gas bubbles containing two or more independently diffusing gases, a topic of considerable importance in the refining of glass melts (Cable [10]), where numerical solution of the differential equations is unavoidable.

This work was undertaken because comparison with Scriven's predictions seemed the soundest way of testing any numerical methods that were developed. This paper confirms the correctness of Scriven's analysis and extends it by solving the equations for the initial transient stage of growth from finite original size and also by applying another test, conservation of the mass of solute transferred across the interface, to both Scriven's solutions and the present numerical methods.

Since electron microscopy became a standard laboratory technique, experimental measurements on growing spheres have not been restricted to sizes much larger than the nucleus. Also particles up to a few micrometres in diameter often remain almost spherical even when larger crystals develop more complex morphology. Knowledge of the transient behaviour of spheres may therefore sometimes be of considerable practical interest. The influence of surface tension often needs to be considered in such cases and is easily introduced into numerical solutions, although it is not treated in this paper.

2. Statement of the problem

Frank [2] pointed out that solutions apply equally well to both heat conduction and mass transfer, but the arguments are presented here only in terms of mass transfer which will generally be slightly more complex.

An isolated sphere of uniform and constant properties is considered in an infinite body of liquid in which there is no flow except for the radial velocity which may result from the change in volume of the system when solute is transferred across the interface. Mass transfer is assumed to be controlled by diffusion in the liquid, equilibrium being always maintained at the interface. Diffusivity is taken to be independent of concentration but the density of the solution may vary; the partial molar volumes of solute and solvent

0022–2461/87 $03.00 + .12

are constant but not necessarily equal. Viscous, inertial and surface tension forces are assumed to have no influence on transport in the liquid or conditions at the interface. Chemical reactions do not complicate the behaviour.

If c_i is the molar concentration of species i and y_i is the volume fraction of that species, we have for only one solute

$$y_1 + y_2 = 1 \quad \text{and} \quad c_i v_i = y_i \quad (i = 1, 2) \tag{1}$$

where v_i is the partial molar volume of that species. The volume average velocity, u, at a point in the liquid must be the sum of the contributions by the solute ($i = 1$) and the solvent ($i = 2$), so that

$$u = y_1 u_1 + (1 - y_1) u_2 \tag{2}$$

For conditions of spherical symmetry the equation of continuity for each component is, if r is radius and t time,

$$\frac{\partial c_i}{\partial t} + \frac{1}{r^2}\frac{\partial}{\partial r}(r^2 u_i c_i) = 0 \qquad i = 1, 2 \tag{3}$$

Taking all of these equations into account leads to

$$\frac{1}{r^2}\frac{\partial}{\partial r}(r^2 u) = 0 \tag{4}$$

from which it follows that the velocity in the liquid outside the sphere is

$$u(r) = (a/r)^2 u(a) \tag{5}$$

where a is the radius of the sphere. As no solvent is transferred across the surface of the sphere (a condition that could be relaxed, see Frank [2]),

$$u_2(a) = \mathrm{d}a/\mathrm{d}t \tag{6}$$

The rate of transfer, J, of the solute into the growing sphere must be given by the difference between the velocity of the solute, $u_1(a)$, and that of the interface itself,

$$J = c_s \frac{\mathrm{d}a}{\mathrm{d}t} = -c_1(a)\left(u_1(a) - \frac{\mathrm{d}a}{\mathrm{d}t}\right) \tag{7}$$

where c_s is the molar concentration of pure solute in the sphere. As c_s is constant,

$$u_1(a) = \left(1 - \frac{c_s}{c_1(a)}\right)\frac{\mathrm{d}a}{\mathrm{d}t} \tag{8}$$

Using Equation 2 and the other above relations gives the velocity of the liquid at the interface to be

$$u(a) = (1 - c_s v_1)\frac{\mathrm{d}a}{\mathrm{d}t}. \tag{9}$$

The diffusive flux into the sphere must be equal to the difference between the velocity of the solution and that of the solute, hence

$$D\left(\frac{\partial c}{\partial r}\right)_a = c_1[u(a) - u_1(a)] \tag{10}$$

where D is the diffusion coefficient. Combination of the last three equations now gives the rate of growth in terms of the diffusive flux as

$$\frac{\mathrm{d}a}{\mathrm{d}t} = \frac{D}{c_s[1 - c_1(a)v_1]}\left(\frac{\partial c}{\partial r}\right)_a \tag{11}$$

It is now necessary to consider the equation describing diffusion in the liquid; an overall material balance for solute reduces to

$$\frac{\partial c}{\partial t} = D\frac{\partial^2 c}{\partial r^2} + \left[\frac{2D}{r} - \varepsilon\left(\frac{a}{r}\right)^2\frac{\mathrm{d}a}{\mathrm{d}t}\right]\frac{\partial c}{\partial r} \tag{12}$$

if $\varepsilon = 1 - c_s v_1$: however, this equation does not require $v_1 = v_2$ as assumed by Scriven. The boundary conditions implied by the assumptions are

$$c(a) = c_a \quad \text{and} \quad c(\infty) = c_\infty \quad t \geqslant 0 \tag{13}$$

3. Analytical solutions

After assuming that $\partial c/\partial t = 0$, Frank [2] solved Equation 12 for the boundary conditions given by Equation 13 for the special case $\varepsilon = 0$, that is $u(r) = 0$, and the range of such solutions was extended by Scriven to the general case $\varepsilon \neq 0$. These authors thus assumed that there was a unique function for

$$c(r, t) = c(s) \tag{14}$$

which required

$$s = \frac{r}{2(Dt)^{1/2}} \tag{15}$$

For growth from zero this gave

$$a = 2\beta(Dt)^{1/2} \tag{16}$$

According to this model the concentration profile is given by

$$c\left(\frac{r}{a}\right) = c_\infty - 2\beta^2 c_s\left[1 - \frac{(1-\varepsilon)}{c_s}\right] \times \int_{1-a/r}^{1} \exp\{\beta^2[1 + 2\varepsilon x - (1 - x)^{-2}]\}\,\mathrm{d}x \tag{17}$$

and, on introducing the boundary conditions, the relation between the solubility parameter ϕ and the growth rate β is

$$\phi = \frac{c_\infty - c_a}{c_s - c_a(1-\varepsilon)} = 2\beta^2 \int_0^1 \exp\{\beta^2[1 + 2\varepsilon x - (1-x)^{-2}]\}\,\mathrm{d}x \tag{18}$$

To confirm the validity of this analysis and to demonstrate the role of the partial molar volumes, conservation of material may be demonstrated as follows. Consider a volume element containing n_1 moles of solute and n_2 moles of solvent which contribute volumes of

$$n_1 v_1 + n_2 v_2 = V \tag{19}$$

As $n_i = c_i V$ by definition, the volume of solvent may be written as

$$v_2 = V(1 - c_1 v_1) = V(1 - y_1) \tag{20}$$

If the content of solute changes from n to n' as a result

of diffusion

$$n - n' = cV - c'V' = \frac{V}{1 - cv_1}\left(\frac{c}{1 - cv_1} - \frac{c'}{1 - c'v_1}\right) \quad (21)$$

and combining the last two equations leads to

$$\frac{n - n'}{V} = \frac{c - c'}{1 - cv_1} = \frac{c - c'}{1 - (1-\varepsilon)c/c_s} \quad (22)$$

Note that this does not require $v_1 = v_2$. Conservation of solute for a sphere growing from zero thus requires that

$$\frac{1}{1 - (1-\varepsilon)c_\infty/c_s}\int_a^\infty 4\pi r^2(c_\infty - c)\,dr = 4\pi a^3 c_s/3 \quad (23)$$

Applying this test to Scriven's solution (Equation 17) leads to the condition

$$G = 6\beta^2 \frac{1 - (1 - \varepsilon)c_a/c_s}{1 - (1 - \varepsilon)c_\infty/c_s}\int_a^\infty \left(\frac{r}{a}\right)^2 \times \int_{1-a/r}^1 \exp\{\beta^2[1 + 2\varepsilon x - (1 - x)^{-2}]\}\,dx\,d(r/a) = 1 \quad (24)$$

A fourth-order Runge–Kutta numerical technique was therefore used to solve

$$I(w) = \int_0^w \exp\{\beta^2[1 + 2\varepsilon x - (1 - x)^{-2}]\}\,dx \quad (25)$$

with $w = 1 - a/r$, the discrete pairs w_j, $I(w_j)$ being used to confirm the validity of Equation 24, that is conservation of mass. This test was made for five values of β covering the range 0.01 to 20 with ε equal to both 0 and 1 in all cases: nine of the results gave $G = 1.000$ and the tenth was 0.998. These results were considered very satisfactory and confirmed the accuracy of the numerical methods used to solve Equations 17 and 25, as well as demonstrating conservation of mass.

4. Numerical solutions for finite initial size

For this purpose it is useful to cast the equations into dimensionless form. The following variables were used,

$$x = \frac{r}{a} \qquad R = \frac{a}{a_0} \qquad z = \frac{Dt}{a_0^2} \qquad F = \frac{c - c_\infty}{c_s - c_a(1 - \varepsilon)} \quad (26)$$

in which a_0 is the initial radius of the sphere. Equation 12 is thus transformed into

$$R^2\frac{\partial F}{\partial z} = \frac{\partial^2 F}{\partial x^2} + \left[\frac{2}{x} + R(x - \varepsilon x^{-2})\frac{dR}{dz}\right]\frac{\partial F}{\partial x} \quad (27)$$

whilst the rate of growth of the sphere (Equation 11) becomes

$$\frac{dR}{dz} = \frac{1}{R}\left(\frac{\partial F}{\partial x}\right)_{x=1} \quad (28)$$

The boundary and initial conditions become

$$F(\infty) = 0 \qquad F(R) = -\phi$$
$$F(x) = 0 \qquad x > 1,\ z = 0 \quad (29)$$

Equation 17 suggests that for large R the solutions should become a function of only $x = r/a$. Transformation of the space variable into x therefore immobilizes the interface and assists convergence of the finite difference solutions by reducing the influence of a second independent variable (time), especially for large R.

The finite difference numerical procedures were based on the truncated series expansion

$$F(x + \delta x) = F(x) + (\delta x)\frac{\partial F}{\partial x} + \tfrac{1}{2}(\delta x)^2\frac{\partial^2 F}{\partial x^2} + \cdots \quad (30)$$

Algorithms were derived to deal with radial intervals of variable amplitude in which the suffixes j and l refer to radial position and time step, respectively. Applying Equation 30 to the three points $(x_j - \delta x_1)$, x_j and $(x_j + \delta x_2)$ yields

$$\frac{\partial F}{\partial x} = \frac{1}{\delta x_1 + \delta x_2} \times \left[\frac{\delta x_1}{\delta x_2}F_{j+1,l} + \left(\frac{\delta x_2}{\delta x_1} - \frac{\delta x_1}{\delta x_2}\right)F_{j,l} - \frac{\delta x_2}{\delta x_1}F_{j-1,l}\right] \quad (31)$$

and

$$\frac{\partial^2 F}{\partial x^2} = \frac{2}{\delta x_1 + \delta x_2} \times \left[\frac{F_{j+1,l}}{\delta x_2} - \left(\frac{1}{\delta x_1} + \frac{1}{\delta x_2}\right)F_{j,l} + \frac{F_{j-1,l}}{\delta x_1}\right] \quad (32)$$

where

$$\delta x_1 = x_j - x_{j-1} \quad \text{and} \quad \delta x_2 = x_{j+1} - x_j \quad (33)$$

Local balances involving two time steps l and $l + 1$ were obtained as an average for the discrete forms of the equations at those time steps, the concentrations $F_{j-1,l+1}$, $F_{j,l+1}$ and $F_{j+1,l+1}$ being expressed as

$$\alpha_{1,j-1}F_{j-1,l+1} + \alpha_{2,j-1}F_{j,l+1} + \alpha_{3,j-1}F_{j+1,l+1} = \alpha_4 \qquad j = 2, 3, \ldots, n - 1 \quad (34)$$

The boundary conditions

$$F_{1,l+1} = F(R) = -\phi \quad \text{and} \quad F_{n,l+1} = F(\infty) = 0 \quad (35)$$

simplify the first and last balances; for $j = 2$ and $j = n - 1$,

$$\alpha_{2,1}F_{2,l+1} + \alpha_{3,1}F_{3,l+1} = \alpha_{4,1} + \phi\alpha_{1,1} \quad (36)$$

and

$$\alpha_{1,n-2}F_{n-2,l+1} + \alpha_{2,n-2}F_{n-1,l+1} = \alpha_{4,n-2} \quad (37)$$

The resulting system of equations was solved by

TABLE I Evolution of growth rates towards the asymptotic regime for the case $\varepsilon = 1$

R	$\beta' = R/(2z^{1/2})$		
	$\phi = 0.01$	$\phi = 1$	$\phi = 100$
2	0.0885	1.745	139.5
5	0.0771	1.378	104.1
10	0.0758	1.336	99.9
10^2	0.0753	1.320	98.3
10^3	0.0753	1.320	98.2
10^5	0.0753	1.320	98.2

the Crank–Nicholson [11] implicit method: implicit methods are usually more stable than explicit ones and prevent the growth of rounding errors or other errors that may arise from the interpolations needed to redistribute the radial mesh points.

The procedures developed for this work included internal optimization of the variable space and time mesh intervals without intervention by the user. This makes the programs simple and economical to use whilst maintaining accuracy. Appropriate algorithms select the time interval according to the time derivative of the radius, and the spacing of the space mesh points is redistributed throughout the process according to the shape of the concentration distribution and the distance that it occupies. Time intervals were defined to obtain a nearly constant relative change of radius ($\Delta a/a$) which is clearly better than using a fixed time interval. A fixed time interval would be likely to give poor accuracy at the beginning and be wasteful of computing time at longer times. Working with a constant change in radius (Δa) is also inefficient, especially for growth to large sizes.

Radial mesh points were distributed to give nearly equal concentration differences near the interface, but in the tail of the profile it was convenient to keep the ratio of adjacent mesh spaces smaller that 1.5. Further details of these criteria and the tests made to justify them have been given by Frade [12].

5. Numerical results

As Equation 16 may be written in dimensionless form as

$$\log R = \log (2\beta) + \tfrac{1}{2} \log z \qquad (38)$$

plotting numerically computed results in logarithmic form allows ready comparison with the predictions of

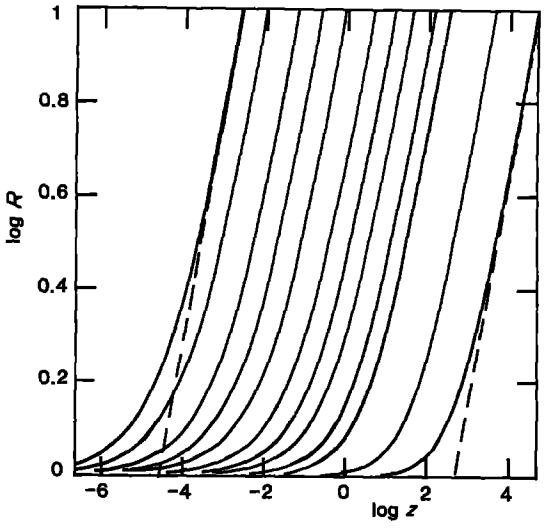

Figure 1 Convergence of growth from finite initial size towards the asymptotic limit for $\varepsilon = 1$ and values of ϕ from 0.001 to 100. The values of ϕ are, from left to right, 100, 50, 20, 10, 5, 2, 1, 0.5, 0.2, 0.1, 0.01 and 0.001. The dashed lines show growth from zero for the largest and smallest values of ϕ.

Scriven's analysis, and this is the most obvious test of the numerical procedures developed. Fig. 1 shows the results of computations for $\varepsilon = 1$ and ϕ from 0.001 to 100 plotted in this way. After an initial transient all the results become parallel straight lines of slope 1/2 as predicted by the analytical model. That the limiting slope is 1/2 may be seen by putting computed pairs of (R, z) data into the dimensionless form of the equation ($R = 2\beta z^{1/2}$) and observing that the values of β obtained (β') do tend to an asymptotic limit (see Table I); continuing the computations to $R = 10^5$ did not require excessive computing times. Table II demonstrates very satisfactory agreement between the asymptotic values of β' obtained from the numerical solutions and those given by Scriven's analysis. Table II records, for wide ranges of the parameters, the values of $\phi(\beta, \varepsilon)$ which the analytical solution produces for the values of β' obtained from the computations for $R = 10^5$. In all cases the two values of ϕ differ by less than 1%; it is unlikely that experimental data would ever exceed this accuracy.

The analytical solution depends on the existence of a unique normalized concentration distribution. Comparison with the evolution of the concentration profiles given by the numerical solutions should

TABLE II Comparisons between finite difference prediction of the asymptotic regime of growth from finite initial size β' and the corresponding analytical predictions $\phi(\beta', \varepsilon)$, for growth from zero size

ϕ	ε					
	0		0.5		1	
	β'	$\phi(\beta', \varepsilon)$	β'	$\phi(\beta', \varepsilon)$	β'	$\phi(\beta', \varepsilon)$
0.001	0.022 84	0.001 002	0.022 83	0.001 002	0.022 83	0.001 002
0.01	0.075 6	0.010 02	0.075 5	0.010 02	0.075 3	0.010 00
0.1	0.282 7	0.100 0	0.277 9	0.100 0	0.273 4	0.100 0
0.95	5.263	0.950 2	–	–	–	–
1	–	–	1.819	1.000	1.320	1.001
1.9	–	–	10.36	1.900	–	–
10	–	–	–	–	10.20	10.01
100	–	–	–	–	98.2	100.1

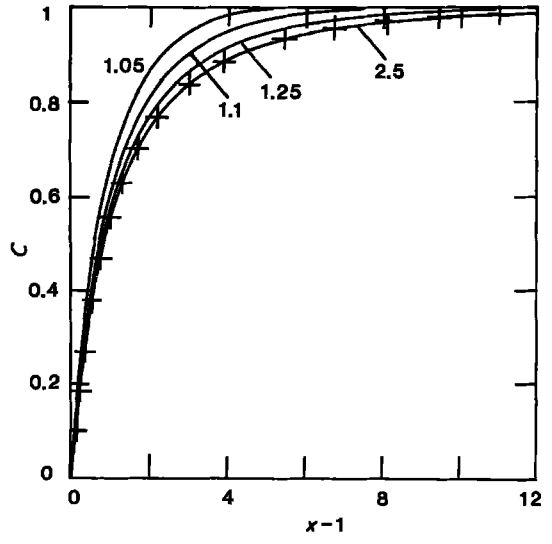

Figure 2 Numerically predicted concentration profiles during growth from finite initial size for $\varepsilon = 1$, $\phi = 0.01$; the numbers show the corresponding values of R and points (++) show Scriven's analytical result. Here $c = (c - c_a)/(c_\infty - c_a)$.

provide further confirmation of the correctness of both. Fig. 2 shows the computed concentration profiles for $\varepsilon = 1$, $\phi = 0.01$ for several values of R from 1.05 to 10; it can be seen that the transformed concentration profiles become independent of time before $R = 2.5$ and are then indistinguishable from that given by Scriven's analysis. Fig. 3 shows a similar comparison for $\varepsilon = 1$, $\phi = 10$; other examples all showed the same behaviour and excellent agreement for the asymptotic profiles.

The agreement found between the asymptotic growth rates and the limiting shapes of the concentration profiles when numerical and analytical predictions are compared is taken to be sufficient evidence that both give valid results for very wide ranges of the relevant parameters (ϕ and ε).

6. Transient growth from finite initial size

Figs 1 to 3 show an initial transient stage affecting both rates of growth and concentration profiles. The

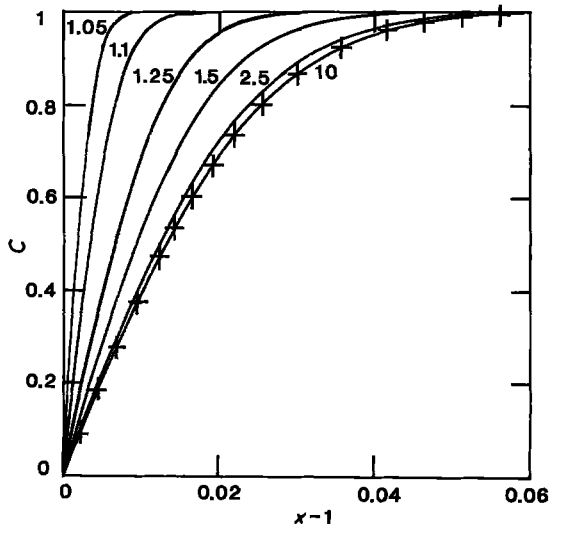

Figure 3 Predicted concentration profiles, as in Fig. 2, for $\varepsilon = 1$, $\phi = 10$.

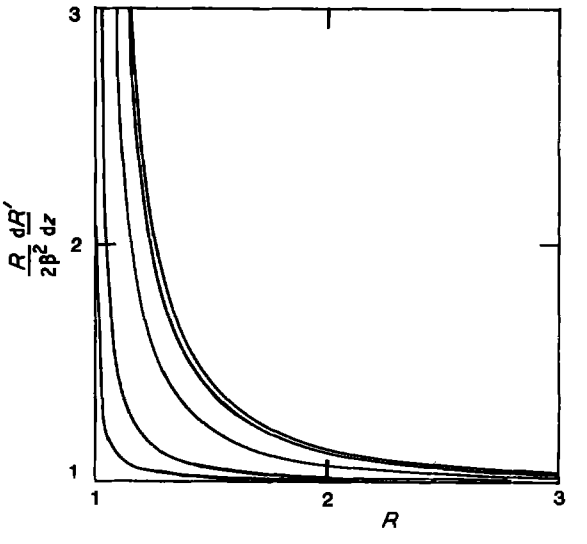

Figure 4 Comparison of rates of growth from finite initial size (dR'/dz) with those for growth from zero ($2\beta^2/R$). The curves are, reading out from the origin, for $\phi = 0.01$, 0.1, 1, 10 and 100.

initial growth from finite size can also be discussed in terms of the rates of growth. According to the equation for growth from zero the rate is given by

$$dR/dz = 2\beta^2/R \qquad (39)$$

The ratio of the computed rate of growth (dR'/dz) to $2\beta^2/R$ thus compares the rates predicted for growth from finite and zero initial sizes. Fig. 4 shows that, during the initial transient stage, growth from finite size is always faster than for growth from zero but the ratio also always approaches unity before the sphere has grown very much. This is due to the singularity imposed by the initial conditions. In terms of size the transient effect is least important for low solubility and increases with solubility. Note, however, that the behaviour has become almost indistinguishable for $\phi = 10$ and 100.

On integrating Equation 39 from $z = 0, R = 1$ one obtains

$$R = 2\beta(z + z_1)^{1/2} \qquad (40)$$

if $z_1 = 1/4\beta^2$. This relation provides another way of comparing the rates of growth from zero and finite initial sizes as shown in Fig. 5. The straight dashed line there shows Equation 40, which can be seen to be a reasonable approximation for small ϕ but it becomes increasingly poorer as ϕ increases. However, results for $\phi > 100$ become indistinguishable from each other when presented in this way. Yet the value of β for the asymptotic regime gives quite good approximations to the entire process for values of ϕ up to 1. For larger ϕ the use of Equation 40 gives appreciable errors, particularly for $R < 2$, and the numerical results should be used.

7. Conclusion

Exact solutions have long been available for describing the diffusion-controlled growth of an isolated sphere from zero initial size. Those solutions have been used to prove the validity of numerical finite difference solutions for growth from finite initial size by comparing both predicted sizes and concentration

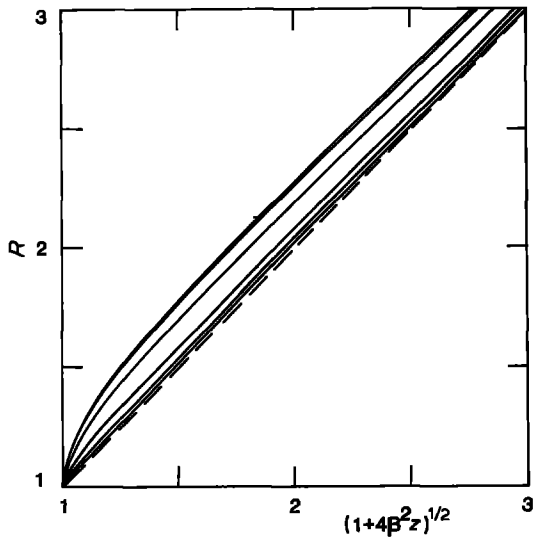

Figure 5 Estimation of growth from finite initial size using the constant β for growth from zero (see text). From the bottom upwards the curves are for ϕ = 0.001, 0.01, 0.1, 1, 10 and 100.

profiles. The concentration profiles for spheres growing from finite size achieve their steady state form for $R > 3$, approximately, and growth rates for the two cases become indistinguishable at the same time. A simple approximation gives generally acceptable predictions for the whole course of growth from finite size for low or moderate solubility ($\phi < 1$) but the numerical results are necessary for higher solubilities.

Analytical solutions are not possible for dissolution of spheres and numerical methods are then necessary. The finite difference techniques reported here were developed with that in mind and should perform equally well for dissolution. Their use for predicting the behaviour of dissolving spheres will be reported separately.

Acknowledgements

The Department of Ceramic Engineering and Glasses, University of Aveiro, Portugal, is thanked for allowing J. R. Frade leave of absence to undertake this work; the Gulbenkian Foundation kindly provided additional financial support.

References

1. H. S. CARSLAW and J. C. JAEGER, "The Conduction of Heat in Solids", 2nd Edn (Clarendon Press, Oxford, 1959) pp. 247–248.
2. F. C. FRANK, *Proc. R. Soc.* **A201** (1950) 586.
3. L. E. SCRIVEN, *Chem. Engng Sci.* **10** (1959) 1.
4. P. S. EPSTEIN and M. S. PLESSET, *J. Chem. Phys.* **18** (1950) 1505.
5. M. CABLE. *Glass Technol.* **1** (1960) 144.
6. R. H. DOREMUS, *J. Amer. Ceram. Soc.* **43** (1960) 655.
7. D. W. READEY and A. R. COOPER, *Chem. Engng Sci.* **21** (1966) 917.
8. M. CABLE and D. J. EVANS, *J. Appl. Phys.* **38** (1967) 2899.
9. J. L. DUDA and J. S. VRENTAS, *Amer. Inst. Chem. Eng. J.* **15** (1969) 351.
10. M. CABLE, in "Glass: Science and Technology", Vol. 2 (Academic Press, New York, 1984) pp. 1–44.
11. J. CRANK and P. NICHOLSON, *Proc. Camb. Phil. Soc.* **43** (1947) 50.
12. J. R. FRADE, PhD thesis, Sheffield University, (1983) pp. 52–85.

Received 17 February
and accepted 28 April 1986